CANCER DISCOVERY

Discovery of a Novel ERK Inhibitor with Activity in Models of Acquired Resistance to BRAF and MEK Inhibitors

Erick J. Morris, Sharda Jha, Clifford R. Restaino, et al.

Cancer Discovery 2013;3:742-750. Published OnlineFirst April 24, 2013.

Published OnlineFirst April 24, 2013; DOI: 10.1158/2159-8290.CD-13-0070

RESEARCH BRIEF

Discovery of a Novel ERK Inhibitor with Activity in Models of Acquired Resistance to BRAF and MEK Inhibitors

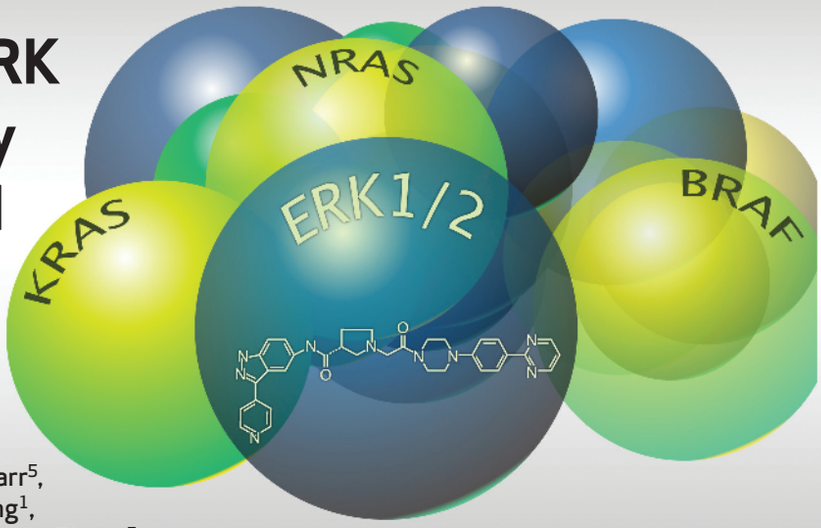

Erick J. Morris[1], Sharda Jha[1], Clifford R. Restaino[1], Priya Dayananth[5], Hugh Zhu[6], Alan Cooper[6], Donna Carr[5], Yongi Deng[2], Weihong Jin[5], Stuart Black[5], Brian Long[1], Jenny Liu[5], Edward DiNunzio[5], William Windsor[5], Rumin Zhang[5], Shuxia Zhao[1], Minilik H. Angagaw[1], Elaine M. Pinheiro[1], Jagdish Desai[6], Li Xiao[6], Gerald Shipps[2], Alan Hruza[5], James Wang[6], Joe Kelly[6], Sunil Paliwal[6], Xiaolei Gao[6], Boga Sobhana Babu[6], Liang Zhu[2], Pierre Daublain[3], Ling Zhang[4], Bart A. Lutterbach[1], Marc R. Pelletier[1], Ulrike Philippar[1], Phieng Siliphaivanh[2], David Witter[2], Paul Kirschmeier[5], W. Robert Bishop[5], Daniel Hicklin[5], D. Gary Gilliland[1], Lata Jayaraman[1], Leigh Zawel[1], Stephen Fawell[1], and Ahmed A. Samatar[1]

ABSTRACT

The high frequency of activating *RAS* or *BRAF* mutations in cancer provides strong rationale for targeting the mitogen-activated protein kinase (MAPK) pathway. Selective BRAF and MAP-ERK kinase (MEK) inhibitors have shown clinical efficacy in patients with melanoma. However, the majority of responses are transient, and resistance is often associated with pathway reactivation of the extracellular signal-regulated kinase (ERK) signaling pathway. Here, we describe the identification and characterization of SCH772984, a novel and selective inhibitor of ERK1/2 that displays behaviors of both type I and type II kinase inhibitors. SCH772984 has nanomolar cellular potency in tumor cells with mutations in *BRAF*, *NRAS*, or *KRAS* and induces tumor regressions in xenograft models at tolerated doses. Importantly, SCH772984 effectively inhibited MAPK signaling and cell proliferation in BRAF or MEK inhibitor–resistant models as well as in tumor cells resistant to concurrent treatment with BRAF and MEK inhibitors. These data support the clinical development of ERK inhibitors for tumors refractory to MAPK inhibitors.

SIGNIFICANCE: BRAF and MEK inhibitors have activity in MAPK-dependent cancers with *BRAF* or *RAS* mutations. However, resistance is associated with pathway alterations resulting in phospho-ERK reactivation. Here, we describe a novel ERK1/2 kinase inhibitor that has antitumor activity in MAPK inhibitor-naïve and MAPK inhibitor-resistant cells containing *BRAF* or *RAS* mutations. *Cancer Discov; 3(7); 742–50. ©2013 AACR.*

See related commentary by Nissan et al., p. 719.

Authors' Affiliations: [1]Discovery Oncology Merck Research Laboratories, [2]Discovery Chemistry Merck Research Laboratories, and [3]Basic Pharmaceutical Sciences, Merck Research Laboratories, Boston, Massachusetts; [4]Department of Clinical Research Oncology, [5]Merck Research Laboratories, Kenilworth; and [6]Department of Chemistry, Merck Research Laboratories, Rahway, New Jersey

Note: Supplementary data for this article are available at Cancer Discovery Online (http://cancerdiscovery.aacrjournals.org/).

Current affiliation for P. Kirschmeier: Belfer Institute for Applied Cancer Science, Dana-Farber Cancer Institute, Boston, Massachusetts.

Current affiliation for S. Fawell: Oncology iScience, AstraZeneca, Waltham, Massachusettts.

Corresponding Author: Ahmed A. Samatar, Merck Research Laboratories, 33 Avenue Louis Pasteur, Boston, MA 02115. Phone: 617-992-3990; Fax: 617-992-2412; E-mail: ahmed.samartar@merck.com or ahmed.samatar95@gmail.com

doi: 10.1158/2159-8290.CD-13-0070

Published OnlineFirst April 24, 2013; DOI: 10.1158/2159-8290.CD-13-0070

INTRODUCTION

Specific inhibitors of RAF and MEK kinases have been developed to target *BRAF*- and *RAS*-mutant tumors (1–6). In particular, the BRAF inhibitor vemurafenib (formerly PLX4032) has been U.S. Food and Drug Administration–approved for the treatment of $BRAF^{V600E}$-mutant metastatic melanoma (7). Although these results are encouraging, durable responses are limited by acquired resistance occurring at a median time of approximately 6 to 7 months (2, 8). The combination of the BRAF inhibitor dabrafenib with the MEK inhibitor trametinib has shown significant clinical benefit in *BRAF*-mutant melanoma compared with BRAF or MEK inhibitor monotherapy (1). Interestingly, BRAF/MEK inhibitor combination treatment has been shown to block phosphorylated extracellular signal-regulated kinase (phospho-ERK) reactivation in melanoma cells (9, 10), a phenomenon that may possibly reduce the emergence of clinical resistance. Mechanisms of resistance to BRAF/MEK combination therapy are currently unknown, but ERK represents an attractive downstream target to exploit. To this end, we developed and characterized SCH772984, a novel, specific inhibitor of ERK1/2 activity, and show robust efficacy in *RAS*- or *BRAF*-mutant cancer cells. Moreover, SCH772984 was also effective in single-agent BRAF or MEK inhibitor resistance as well as in cells that became resistant to the combination of these agents.

RESULTS

A selective ERK inhibitor was identified using an affinity-based mass spectroscopy high-throughput platform (11). A library of approximately 5 million compounds was screened for binding to the unphosphorylated form of the ERK2 protein. Synthetic chemistry efforts improved enzymatic potency and selectivity, culminating in the synthesis of the ATP-competitive compound SCH772984 (Fig. 1A). SCH772984 potently inhibited ERK1 and ERK2 activity with IC_{50} values of 4 and 1 nmol/L, respectively (Fig. 1B). SCH772984 is highly selective, with only seven kinases of 300 tested showing more than 50% inhibition at a concentration of 1 μmol/L (Supplementary Table S1).

Treatment of the $BRAF^{V600E}$-mutant human melanoma cell line LOXIMV1 (LOX) with SCH772984 resulted in a dose-dependent inhibition of phosphorylation of the ERK substrate p90 ribosomal S6 kinase (T359/S363 phospho-RSK; Fig. 1C). Unexpectedly, SCH772984 also inhibited phosphorylation of residues in the activation loop of ERK itself

A

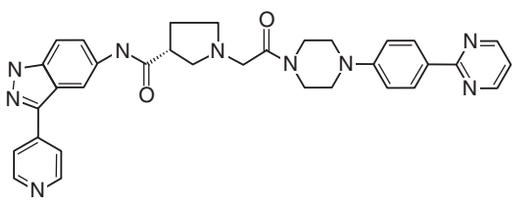

B

SCH772984 inhibition of *in vitro* kinase activity

Kinase	IC_{50} (μM)
ERK2	0.001
ERK1	0.004
MEK1	>10

C

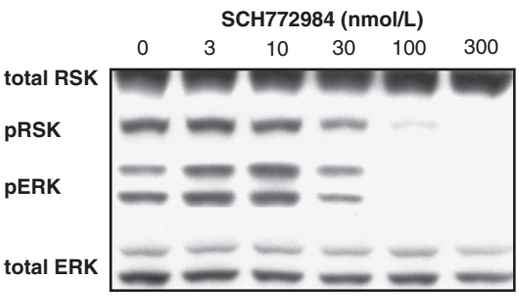

D

TdF Binding	ERK		pERK		MEK	
Compound	K_D (nmol/L)	TM	K_D (nmol/L)	TM	K_D (nmol/L)	TM
GSK1120212	No binding	–0.15 ± 0.20	No binding	0.23 ± 0.32	7 ± 2.7	8.0 ± 0.51
SCH772984	0.24 ± 0.4	10.3 ± 0.30	0.19 ± 0.12	9.8 ± 0.23	No binding	–0.17 ± 0.41
VTX-11e	5.4 ± 2.2	6.8 ± 1.3	0.11 ± 0.62	10.3 ± 1.3	No binding	–0.1 ± 0.3

E

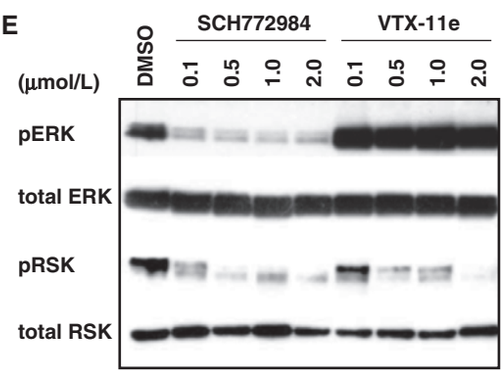

Figure 1. Biochemical and cell-based activity of SCH772984. **A,** chemical structure of SCH772984. **B,** effects of SCH772984 on kinase activity of ERK1, ERK2, and MEK1. **C,** SCH772984 inhibits ERK and RSK phosphorylation. LOX $BRAF^{V600E}$ melanoma cells were treated with increasing concentrations of SCH772984 for 24 hours, and lysates were subjected to Western blot analysis using antibodies against phosphorylated ERK1/2 (pERK), phosphorylated p90 ribosomal S6 kinase (pRSK), total ERK, or total RSK. **D,** TdF binding activity of SCH772984, VTX-11e, or GSK1120212 to recombinant ERK2 and MEK1 enzymes. **E,** target engagement on pERK/pRSK for SCH772984 versus VTX-11e in *BRAF*-mutant A375 cells treated for 4 hours. TdF, temperature-dependent fluorescence.

Published OnlineFirst April 24, 2013; DOI: 10.1158/2159-8290.CD-13-0070

(T202/Y204 and T185/Y187 of ERK1 and ERK2, respectively), a modification catalyzed by the ERK-activating kinases, MEK 1 and MEK 2. This latter observation was unexpected given that SCH772984 did not directly inhibit MEK1, MEK2, BRAF, or CRAF enzyme activity (Fig. 1B; Supplementary Table S1). To further rule out a direct interaction between SCH772984 and MEK, the binding of SCH772984 to MEK1 (or ERK2 as a positive control) was evaluated biophysically using a temperature-dependent fluorescence (TdF) assay (Fig. 1D and Supplementary Fig. S1). As a control, the allosteric MEK inhibitor GSK1120212 specifically bound MEK1. Consistent with results from the kinase panel, SCH772984 bound both purified unphosphorylated and phosphorylated ERK2 proteins but did not bind to purified MEK1.

To further elucidate the mechanism of action of SCH772984, we compared its mitogen-activated protein kinase (MAPK) pathway inhibition with that of the previously described ATP-competitive ERK inhibitor VTX-11e (12, 13). In the *BRAF*^{V600E}-mutant A375 melanoma cell line, both compounds inhibited the formation of phospho-RSK in a dose-dependent manner (Fig. 1E). Interestingly, and in contrast to the inhibition of phospho-ERK seen with SCH772984, phospho-ERK increased in cells treated with VTX-11e. VTX-11e–mediated reactivation of phospho-ERK is likely due to feedback activation as previously described (reviewed in ref. 14). Increased ERK phosphorylation was similarly observed following PLX4032 treatment in *KRAS*-mutant cell lines (Supplementary Fig. S2). This was abolished by treatment with SCH772984 confirming that SCH772984 prevents MEK-mediated ERK phosphorylation. Interestingly, although the inhibition of phospho-ERK and phospho-RSK by SCH772984 was sustained for 24 hours, by 36 hours, the inhibition of phospho-ERK was lost, whereas the inhibition of phospho-RSK was maintained (Supplementary Fig. S3). Further pathway analysis showed that SCH772984 reduced pCRAF S289/S296/S301 phosphorylation (direct ERK phosphorylation sites that inhibit CRAF activity; ref. 15), suggesting that rebound ERK phosphorylation is a result of CRAF upregulation. Taken together, we hypothesize that, in addition to ATP-competitive inhibition of ERK1/2 catalytic activity, SCH772984 induces or stabilizes a conformational state in ERK that prevents activation by MEK, and this is sufficient to maintain ERK inhibition even in the presence of feedback signaling by CRAF.

The studies described above established SCH772984 as a potent inhibitor of ERK in *BRAF*- and *KRAS*-mutant cells. To determine the selectivity of SCH772984 in these contexts, we assessed *in vitro* antiproliferative activity in a panel of 121 human tumor cell lines (Fig. 2A, Supplementary Fig. S4, and Supplementary Table S2). SCH772984 showed EC_{50} values less than 500 nmol/L (defined as responders) in approximately 88% and 49% of *BRAF*-mutant ($n = 25$) or *RAS*-mutant ($n = 35$) tumor lines, respectively (Fig. 2A). Flow cytometric analysis of SCH772984-sensitive melanoma cells revealed a G_1 arrest as well as an increase in the sub-G_1 fraction indicative of apoptosis (Supplementary Fig. S5). Less than 20% of cells wild-type for both *RAS* and *BRAF* ($n = 61$) were sensitive to SCH772984 (Fig. 2A).

In vivo antitumor efficacy of SCH772984 was evaluated in *BRAF*- or *KRAS*-mutant xenograft models established from human melanoma or pancreatic carcinoma cell lines. Treatment of *BRAF*-mutant LOX melanoma xenografts with SCH772984 (50 mg/kg twice daily) led to 98% tumor regression (Fig. 2B). Dose-dependent antitumor activity was also observed in the *KRAS*-mutant pancreatic MiaPaCa model, with 36% regression at 50 mg/kg twice daily (Fig. 2C). Importantly, tumor regression was accompanied by robust inhibition of ERK phosphorylation in tumor tissue (Fig. 2D). SCH772984 was well tolerated on this schedule as measured by morbidity, lethality, or body weight loss (Fig. 2E).

MAPK inhibitors are currently in development for *BRAF*- and *RAS*-mutant cancers, and the BRAF inhibitor vemurafenib (PLX4032) is approved for the treatment of *BRAF*-mutant metastatic melanoma. Despite impressive initial clinical responses to MAPK inhibitors, most patients relapse (reviewed in ref. 16). To determine whether SCH772984 was efficacious in models of BRAF or MEK inhibitor resistance, we generated *BRAF*-mutant melanoma or *KRAS*-mutant colorectal cancer cell lines resistant to the BRAF inhibitor PLX4032 or the MEK inhibitor GSK1120212, respectively. Cell lines were serially passaged in the presence of escalating concentrations of compound over a period of 4 to 8 months. Cell line pools became resistant to high-dose PLX4032 (10 μmol/L) or GSK1120212 (1 μmol/L), as evidenced by robust proliferation in the presence of inhibitor (data not shown). Acquired activating mutations in *KRAS*^{G13D} or *NRAS*^{G12C} were identified in PLX4032-resistant *BRAF*-mutant A375 melanoma (Fig. 3A and B) or PLX4032-resistant *BRAF*-mutant RKO colorectal (Supplementary Fig. S6) lines, respectively. GSK1120212 resistance was associated with acquired mutations in *MEK1* (*MEK1*^{V211D} mutation in *BRAF*-mutant RKO and *MEK1*$^{G128D/L215P}$ mutations in *KRAS*-mutant HCT116; Fig. 3C), consistent with previously described alleles that confer AZD6244 resistance (17). Acquisition of drug resistance was accompanied by pathway reactivation as indicated by increased baseline phospho-ERK levels (Fig. 3B) and increased transcription of *DUSP6*, *MYC*, *LIF*, and *IL8*, well-known MAPK target genes (Supplementary Fig. S7). SCH772984 showed potent growth inhibition in all of the resistant models described above, with IC_{50} values similar to those observed in parental lines (Fig. 3 and Supplementary Fig. S6). As expected, phospho-ERK, phospho-RSK, and mRNA levels for *DUSP6*, *MYC*, *LIF*, and *IL8* were all decreased following SCH772984 treatment (Figs. 3B and Supplementary Fig. S7).

BRAF amplification as well as expression of drug-resistant *BRAF* splice-variants lacking N-terminal regulatory regions have been described as clinical resistance mechanisms in patients with PLX4032-relapsed melanoma, whereas *MEK1*^{P124L} was identified in a patient who relapsed on treatment with the MEK inhibitor AZD6244 (10, 17–19). Importantly, *BRAF* amplification has been shown to mediate cross-resistance to MEK inhibitors (10), whereas *MEK* mutations mediate cross-resistance to BRAF inhibitors (17, 20). To test whether ERK blockade was efficacious in the context of these clinically observed resistance mechanisms, stable cell lines expressing each of these variants were engineered in a *BRAF*^{V600E} A375 background. As shown in Fig. 3D, overexpression of *KRAS*^{G13D} (positive control), *BRAF*^{V600E} (to simulate amplification), or *BRAFV600*$^{E\Delta 2\text{-}8}$ all conferred resistance to PLX4032, whereas overexpression of *MEK1*^{P124L} (residue proximal to

Published OnlineFirst April 24, 2013; DOI: 10.1158/2159-8290.CD-13-0070

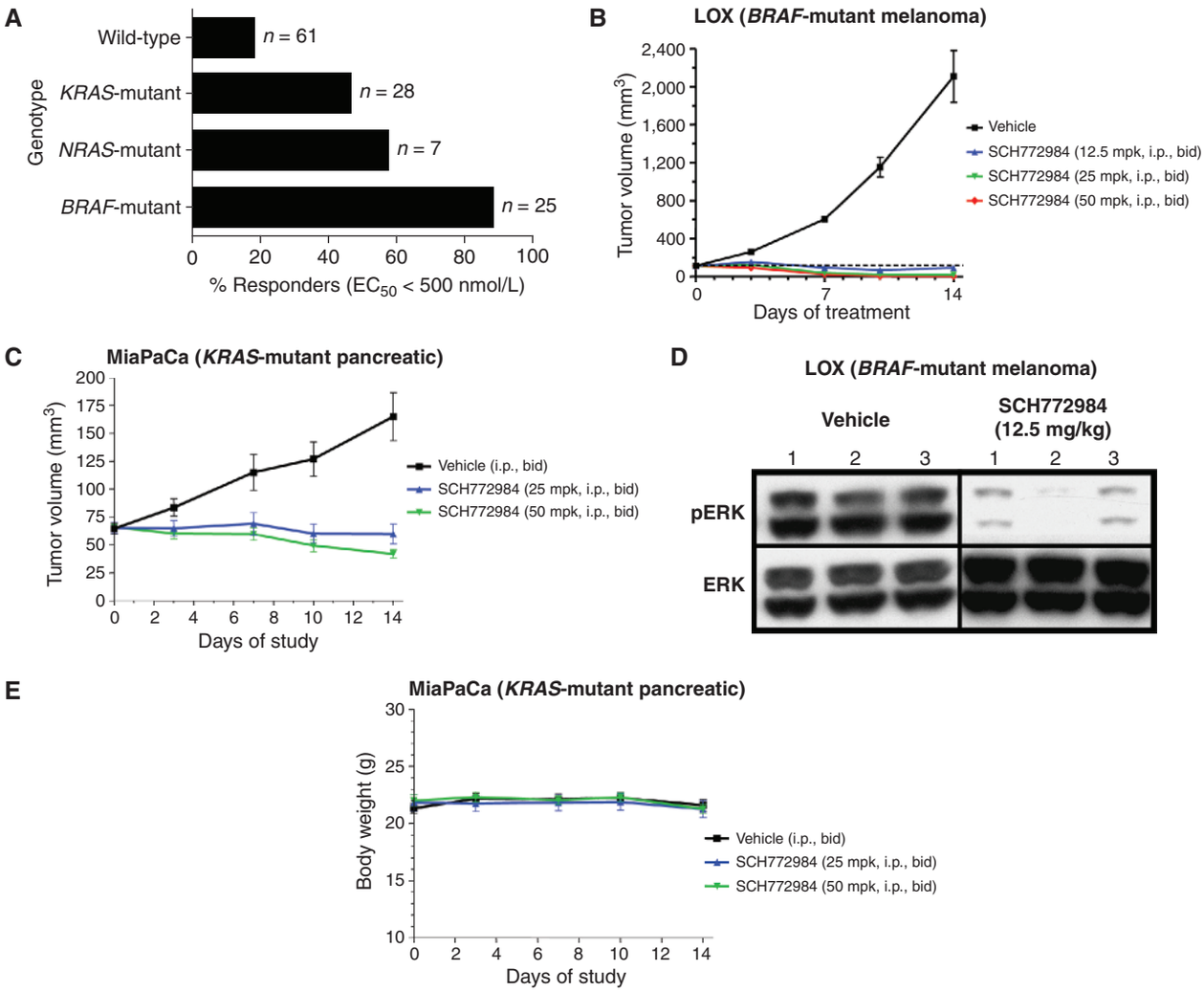

Figure 2. SCH772984 is efficacious in *BRAF*- or *RAS*-mutant tumor cells. **A,** *in vitro* activity of SCH772984 in a panel of human tumor cell lines (summary of primary data from Supplementary Fig. S3). **B,** *in vivo* activity of SCH772984 in human LOX *BRAF*-mutant melanoma xenograft model. Female nude mice bearing human LOX $BRAF^{V600E}$ tumors more than 100 mm^3 in size were dosed twice daily with vehicle or SCH772984 (12.5, 25, or 50 mg/kg) for 14 days ($n = 10$/group). Dosing occurred from day 1 to day 14. Tumor volume was measured and growth curves were derived from the mean tumor volume in each dose. The percent change in volume is shown after 14 days. Tumor regressions were observed at all doses (17% at 12.5 mg/kg, 84% at 25 mg/kg, and 98% at 50 mg/kg). **C,** *in vivo* activity of SCH772984 in human MiaPaCa *KRAS*-mutant pancreatic xenograft model. Mice were dosed twice daily with vehicle or with 25 mg/kg or 50 mg/kg of SCH772984. Tumor regressions were observed at both doses (9% tumor regression at 25 mg/kg and 36% tumor regression at 50 mg/kg dose). **D,** target engagement of SCH772984 on phospho-ERK in LOX melanoma xenograft tumors. On day 14 after the last dose (6 hours) of 12.5 mg/kg of SCH772984 (lanes 4–5) or vehicle (lanes 1–3), LOX xenograft tumors were harvested (three mice/group) and homogenates from excised tumors were probed for phospho-ERK1/2 and total ERK1/2 levels by Western blots. **E,** body weights of female nude mice with SCH772984 relative to control animals (in MiaPaCa xenograft). No drug related lethality was observed at all doses. mpk, mg/kg; bid, twice daily.

N-terminal negative inhibitory domain) conferred resistance to GSK1120212. In addition, expression of $MEK1^{F129L}$ (allosteric binding site mutant with enhanced activity; refs. 17, 21) or $MEK1^{DD}$ (constitutively active mutant with aspartic acid replacement of activating loop serine residues; ref. 17) all mediated resistance to PLX4032 (Supplementary Fig. S8). Treatment with SCH772984 was efficacious in all contexts described above, suggesting that cells that circumvent BRAF or MEK inhibitor therapy and reactivate ERK signaling remain dependent on ERK.

In a recent clinical study, the combination of a BRAF inhibitor with a MEK inhibitor doubled the progression-free survival benefit relative to either monotherapy (1). As this combination could potentially become the standard-of-care for $BRAF^{V600E}$ melanoma, we sought to develop melanoma models resistant to BRAF/MEK double blockade and evaluate their responsiveness to ERK inhibition. $BRAF^{V600E}$-containing A101D melanoma cells were double-selected with PLX4032 and GSK1120212 until resistant cells proliferated at similar rates compared with parental (Fig. 4A). BRAF and MEK inhibitor combination resistance led to strong reactivation of the MAPK pathway as measured by phospho-ERK and phospho-RSK, either in the presence or absence of both compounds (Fig. 4B). SCH772984

Published OnlineFirst April 24, 2013; DOI: 10.1158/2159-8290.CD-13-0070

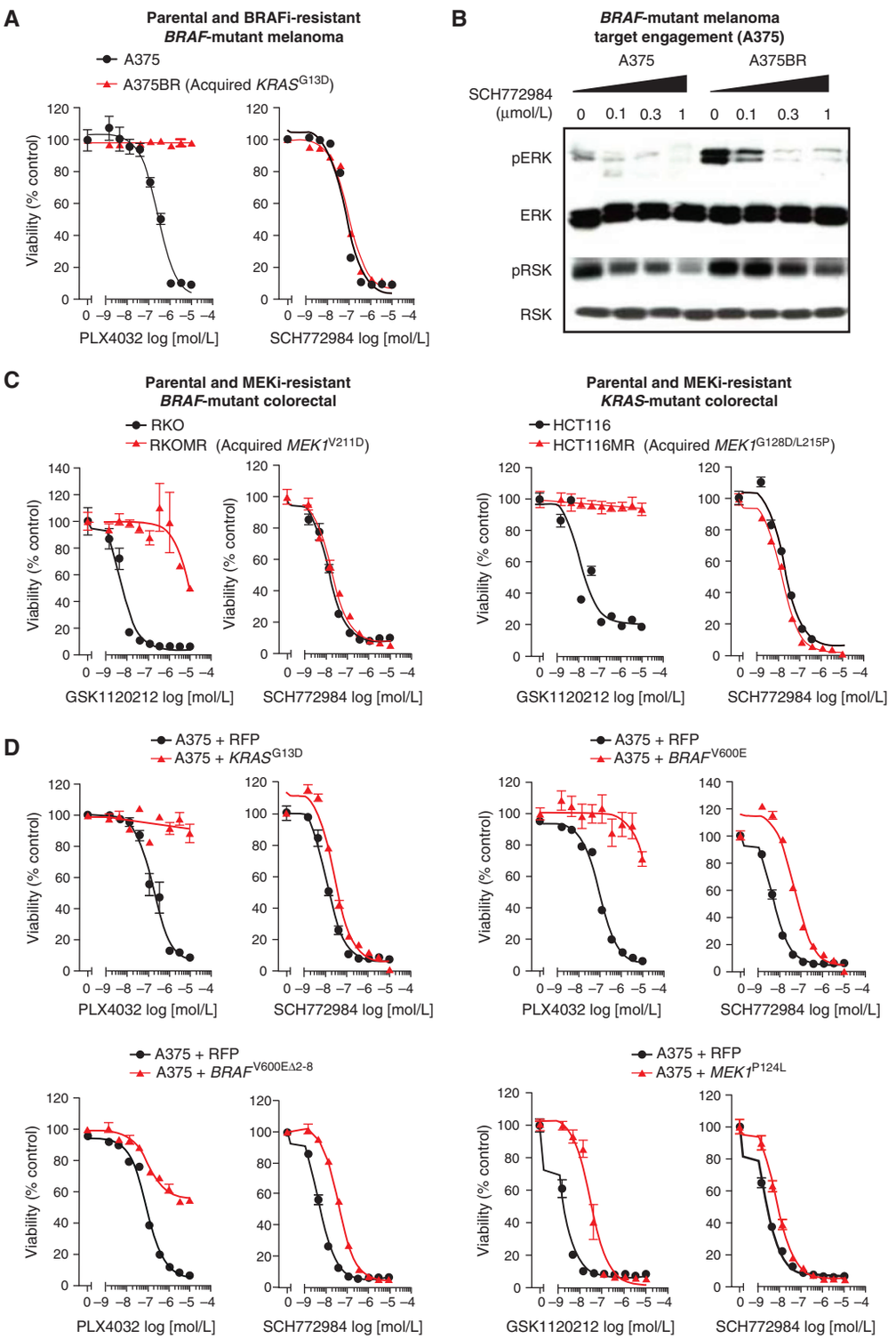

Figure 3. SCH772984 is efficacious in tumor cell lines refractory to either BRAF or MEK inhibitors. **A,** SCH772984 is equally potent in naïve or PLX4032-resistant, *BRAF*-mutant A375 melanoma cells (A375BR). **B,** SCH772984 potently inhibits phospho-ERK (pERK) and phospho-RSK (pRSK) in naïve and PLX4032-resistant *BRAF*-mutant A375 melanoma cells. **C,** SCH772984 is equally potent in naïve or GSK1120212-resistant, *BRAF*-mutant RKO colorectal cancer cells (RKOMR) or *KRAS*-mutant HCT116 colorectal cancer cells (HCT116MR). **D,** SCH772984 is efficacious in *BRAF*-mutant melanoma cells engineered to express various clinically relevant BRAF or MEK inhibitor resistance mechanisms. The ectopic expression of $KRAS^{G13D}$ (as positive control), $BRAF^{V600E}$, or $BRAF^{V600E\Delta 2\text{-}8}$, but not red fluorescence protein (RFP, as negative control), induces resistance to PLX4032. Ectopic expression of $MEK1^{P124L}$ induces resistance to GSK1120212. In all cases, little to no cross-resistance was observed with SCH772984. Cells were treated for 5 days followed by ViaLight assay. Overexpression of each was confirmed by Western blot analysis (data not shown). All data are depicted as mean ± SE ($N = 6$).

Published OnlineFirst April 24, 2013; DOI: 10.1158/2159-8290.CD-13-0070

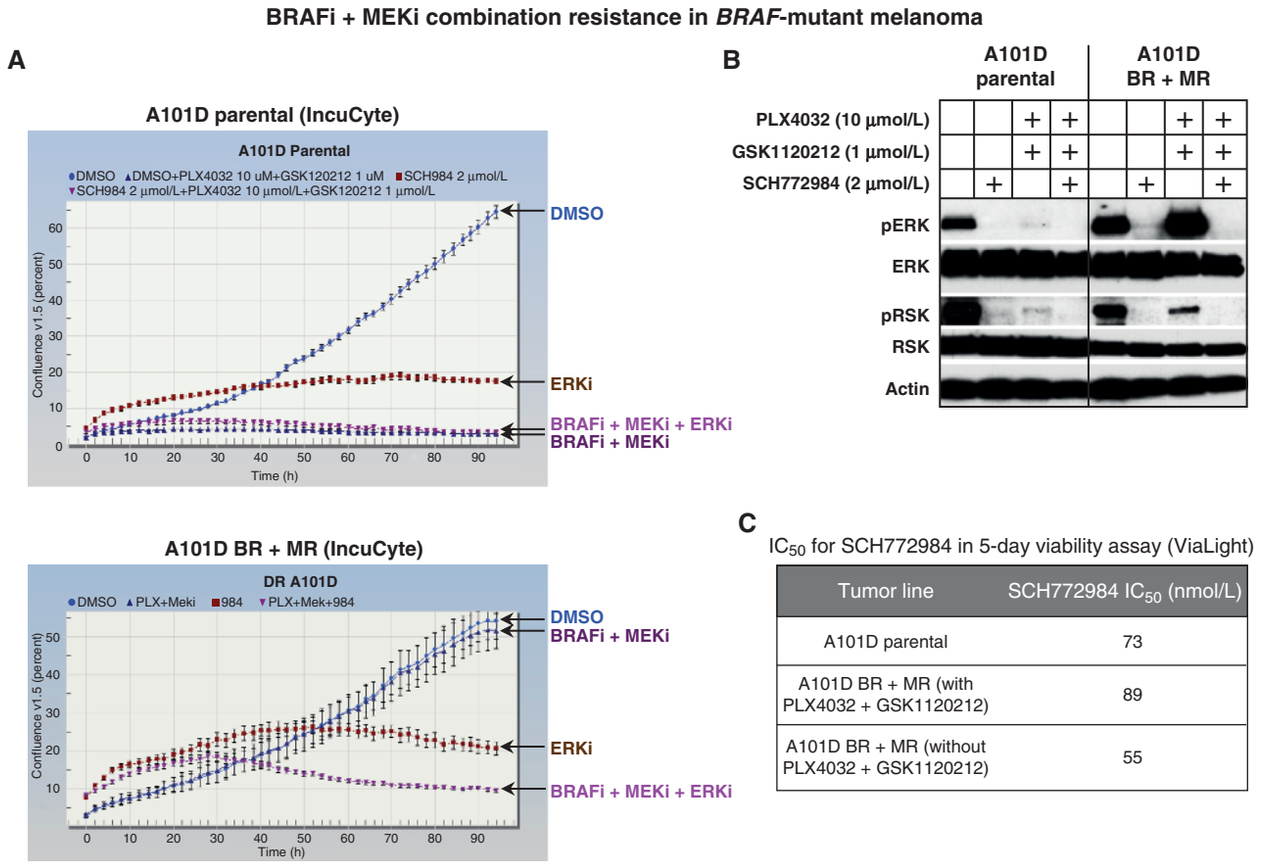

Tumor line	SCH772984 IC_{50} (nmol/L)
A101D parental	73
A101D BR + MR (with PLX4032 + GSK1120212)	89
A101D BR + MR (without PLX4032 + GSK1120212)	55

Figure 4. SCH772984 is efficacious in BRAF and MEK combination resistance in *BRAF*-mutant A101D melanoma cells. **A,** IncuCyte analysis of real time growth confluence (imaged every 2 hours) of parental and A101D BR + MR cells shows similar growth rates despite the presence of high concentrations of PLX4032 (10 µmol/L) and GSK1120212 (1 µmol/L). Treatment with SCH772984 (either alone or in combination with BRAF + MEK inhibitor) is efficacious in both naïve and resistant lines. **B,** A101D BR + MR cells acquire ERK pathway reactivation which is inhibited by SCH772984 (both in the presence and absence of the BRAF/MEK inhibitor combination during the experiment). **C,** SCH772984 treatment IC_{50} values on 5-day ViaLight viability assays for A101D parental and A101D BR + MR cells (both in the presence or absence of BRAF/MEK combination during initial plating; 10 µmol/L PLX4032 + 1 µmol/L GSK1120212). Data are derived from 10-point dose titrations as described in Methods with all data depicted as mean ± SE ($N = 6$).

effectively reduced phospho-ERK/phospho-RSK (Fig. 4B) and inhibited proliferation in the dually resistant A101D melanoma cells in the presence or absence of both BRAF and MEK inhibitors with IC_{50} values similar to the parental line (Fig. 4A and C). Similar results were obtained with the BRAF/MEK inhibitor combination-resistant *BRAF*-mutant RKO colorectal line (Supplementary Fig. S9).

MAPK pathway mutational analysis of parental and dual-resistant lines identified acquired *NRAS*^{G12C}, *MEK1*^{V211D}, and *MEK1*^{L215P} mutations in PLX4032-resistant RKO cells consistent with MAPK pathway reactivation (Supplementary Fig. S9). Interestingly, dual-resistant A101D cells did not acquire mutations in *BRAF*, *HRAS*, *NRAS*, *KRAS*, *MAP2K1* (MEK1), *MAP2K2* (MEK2), *MAPK1* (ERK2), or *MAPK3* (ERK1) in all coding exons analyzed (see Methods). However, in addition to strong ERK reactivation (Fig. 4), we also identified upregulation of BRAF, CRAF, PDGFRB, IGF1RB, and phospho-AKT in this line (Supplementary Fig. S10) consistent with previous reported resistance mechanisms for vemurafenib as well as cross-resistance mechanisms for MEK inhibitors. Taken together, these results suggest that ERK inhibitors such as SCH772984 could be beneficial for BRAF and MEK inhibitor refractory disease with ERK reactivation.

DISCUSSION

Targeted drug therapy in biomarker-selected patient populations is gaining broad acceptance as an effective way to treat cancer based on the inherent genetics of the tumor. Toward that end, SCH772984, a potent and selective ERK inhibitor, was developed for treating malignancies dependent on dysregulated MAPK signaling. Our data implicate ERK inhibition as a therapeutic option for the treatment of patients with *BRAF*-, *KRAS*-, or *NRAS*-mutant tumors, including patients who relapse on BRAF or MEK inhibitor therapy.

SCH772984 possessed strong, preferential activity in a large panel of biomarker-positive (i.e., *BRAF*-, *KRAS*-, and *NRAS*-mutant) cell lines *in vitro* and also produced *in vivo* tumor regressions in xenograft models. Like other MAPK inhibitors, SCH772984 showed broader activity in a panel of *BRAF*-mutant cells than in *KRAS* or *NRAS* mutants. This was expected given the known importance of MAPK signaling

Published OnlineFirst April 24, 2013; DOI: 10.1158/2159-8290.CD-13-0070

downstream of activated BRAF. However, in the future, it will be important to understand why some *RAS*-mutant cells are naturally more resistant to SCH772984, as these mechanisms could limit its clinical use.

It certain contexts, it has been shown that RAF inhibitor efficacy can be limited by ERK reactivation that occurs within 24 hours (22). As SCH772984 effectively inhibited both ERK enzymatic activity as well as its phosphorylation by MEK, we wondered whether SCH772984 might have the ability to block ERK phosphorylation in the context of negative feedback pathway activation. Like vemurafenib, SCH772984 induced rebound signaling kinetics. MAPK signaling was nearly completely eliminated through the initial 24 hours of compound treatment. Thereafter, a loss of ERK-mediated inhibitory CRAF phosphorylation (S289/S296/S301; ref. 15) was observed, as well as dramatic increases in phospho-ERK. Despite negative feedback activation up to and including phospho-ERK, SCH772984 maintained a signaling blockade between ERK and RSK. These results suggest that SCH772984 has a stronger ability to inhibit ERK catalytic activity than MEK phosphorylation of ERK (which was apparently overwhelmed in this setting). Furthermore, this durable inhibition of pRSK in the context of negative feedback favorably distinguishes SCH772984 from BRAF inhibitors.

While tumors can take multiple paths to RAF inhibitor resistance, one common feature seems to be the reactivation of the ERK pathway. Because of its ability to inhibit at a distinct, downstream intervention point in the MAPK pathway, SCH772984 has the potential to overcome resistance induced by MEK or BRAF inhibitors. We examined SCH772984 in various models of previously described, clinically relevant BRAF or MEK inhibitor resistance, including acquired *RAS* mutations, acquired *MEK1* mutations, overexpression of $BRAF^{V600E}$, or a splice-variant lacking an amino-terminal RAS-binding domain, as well as ectopic expression of various *MEK1* mutants (including constitutively active). In all scenarios tested, SCH772984 treatment produced IC_{50} values in viability assays similar to what was observed in parental cells. One exception was the overexpression of either $BRAF^{V600E}$ or a $BRAF^{V600E}$ splice-variant lacking exons 2 to 8 (insensitive to vemurafenib inhibition due to constitutive dimerization), whereby we observed an approximately tenfold IC_{50} shift toward cross-resistance. Currently, the mechanism responsible for this low-level cross-resistance is unknown and further study is necessary. However, when we attempted to hyperactivate ERK to high levels (i.e., overexpression of constitutively active MEK1), we observed little no cross-resistance. This suggests that the ERK node may represent a rate-limiting step within the MAPK pathway that is subject to less fluctuation with regard to biologic signaling (and hence less potential for an IC_{50} shift during cross-resistance). For these reasons, targeting ERK may be more effective than targeting MEK, especially in light of evidence suggesting limited clinical trametinib activity in BRAF inhibitor–refractory melanoma (23).

Development of effective combination strategies is expected to reduce the incidence of clinical resistance that is common with single-agent targeted therapies. The combination of BRAF and MEK inhibition in *BRAF*-mutant melanoma is a good example of the clinical benefit that can be obtained from this approach. Although the clinical mechanisms of resistance to these combinations are largely unknown, we expect that multiple mechanisms resulting in pathway reactivation, or perhaps a single downstream mechanism, might be sufficient for tumor escape. In this study, we show phospho-ERK reactivation in two models of BRAF and MEK combination therapy resistance. SCH772984 was effective in blocking proliferation in both models. Interestingly, in one model, the dual-resistant cells did not acquire mutations in the MAPK pathway but rather upregulated known RTKs previously described to mediate PLX4032 resistance as well as cross-resistance to MEK inhibitors (i.e., PDGFRB; ref. 24). Acquired RTK activation in dual-resistant A101D cells was accompanied by both phospho-ERK and phospho-AKT activation. However, this cell line was still dependent on ERK signaling, as shown by its upregulation of BRAF and CRAF as well as its response to SCH772984. Taken together, our results suggest that clinical resistance to BRAF/MEK combination therapy will likely involve multiple mechanisms resulting in ERK pathway reactivation. Moreover, our data indicate that these mechanisms will likely be similar to those reported to mediate resistance to BRAF or MEK as single agents.

Given that ERK is directly downstream of BRAF and MEK, targeting the MAPK pathway at the level of ERK might offer unique advantages in a variety of MAPK resistance settings. Moreover, ERK directly signals to more than 100 known cellular proteins that are important for tumor cell proliferation, survival, and apoptosis (e.g., pRSK, MYC, BIM). It will be important to define the optimal point of intervention in this critical signaling pathway to aid the development of effective therapeutics for *BRAF*- and *RAS*-mutant cancers. SCH772984 and related compounds provide potent and selective tools to help address this question either alone or in combination with other MAPK inhibitors.

METHODS

Cell Lines and Treatments

For resistant cell line creation, cells were grown in Dulbecco's Modified Eagle Medium with 10% heat-inactivated FBS media and increasing concentrations of inhibitor (PLX4032, 0.1–10 μmol/L; GSK1120212, 0.01–1 μmol/L) over approximately 4 to 8 months until resistant cells acquired growth properties similar to naïve parental cells (at their top drug concentrations). For combination resistance, cells were incubated as above but with alternative dose escalation until a top concentration was acquired (PLX4032 10 μmol/L and GSK1120212 1 μmol/L). The identities of all cell lines used for these studies were confirmed using short tandem repeat DNA analysis at the American Type Culture Collection. Stocks and dilutions of PLX4032, GSK1120212, and SCH772984 were made in dimethyl sulfoxide (DMSO) solvent. Cell proliferation experiments were carried out in a 96-well format (six replicates), and cells were plated at a density of 4,000 cells per well. At 24 hours after cell seeding, cells were treated with DMSO or a 9-point IC_{50} dilution (0.001–10 μmol/L) at a final concentration of 1% DMSO for all concentrations. Viability was assayed 5 days after dosing using the ViaLight luminescence kit (Lonza) following the manufacturer's recommendations ($n = 6$, mean ± SE). For the cell line panel viability assay, cells were treated with SCH772984 for 4 days and assayed by the CellTiterGlo luminescent cell viability assay (Promega). For IncuCyte analysis, cells were plated as above in 96-well plates, and image-based cell confluence data were collected every 2 hours during live growth. For engineered resistant lines, cells were infected with lentivirus produced from lentiORF constructs (pLOC vector) expressing either RFP, $KRAS^{G13D}$, $BRAF^{V600E}$, truncated $BRAF^{V600E}$ lacking exons

Published OnlineFirst April 24, 2013; DOI: 10.1158/2159-8290.CD-13-0070

2–8 (Δ2-8), *MEK1*^{P124L}, *MEK1*^{F129L}, or constitutively active *MEK1*^{DD} (S218D+S222D). Cells were selected in blasticidin (20 μg/mL) and used for ViaLight assays as described above.

Genomic DNA Sequencing

Primer extension sequencing was conducted by GENEWIZ, Inc. using Applied Biosystems BigDye version 3.1. The reactions were then run on Applied Biosystem's 3730xl DNA Analyzer for sequencing of all coding exons in *KRAS*, *HRAS*, *NRAS*, *MAP2K1* (MEK1), *MAP2K2* (MEK2), *MAPK1* (ERK2), *MAPK3* (ERK1), or *BRAF* (coding exon 6 and 11–15).

Total RNA Extraction and cDNA Synthesis

Treated cells were collected with lysis buffer and extraction of RNA was conducted using the RNAeasy mini Kit (Ambion) as per the manufacturer's directions. RNA samples were eluted in 50 μL of nuclease-free water. cDNA was generated from 2 μg of RNA by using a murine MLV reverse transcriptase first-strand cDNA synthesis kit (Applied Biosystems).

Real-Time PCR for MAPK Gene Expression

PCR reactions were conducted and monitored using an ABI Prism 7900 Sequence Detection system (Applied Biosystems). The PCR master mix was based on AmpliTaq Gold DNA polymerase; cDNA samples were analyzed in duplicate. Primers and probes were used at concentrations of 100 and 125 nmol/L per reaction, respectively. After an initial denaturation step of 95°C for 10 minutes, the cDNA products were amplified with 40 PCR cycles (denaturation: 95°C for 15 seconds; extension: 60°C for 1 minute). For each sample, the C_t value was determined as the cycle number at which the fluorescence intensity reached 0.05; this value was chosen after confirming that all curves were in the exponential phase of amplification in this range. Relative expression was calculated using the delta-C_t method using the following equations: ΔC_t (Sample) = C_t (Target) − C_t (Reference); relative quantity = $2^{-\Delta C_t}$. Differentially expressed genes were identified using significance analysis. For each cDNA sample, the Ct value of each target sequence was normalized to the reference genes (*GAPDH*, *TUBULIN*, and *ACTIN*). Primer sets were obtained from Applied Biosystems for the following genes: *DUSP6* (Hs00737962), *MYC* (Hs00905030), *LIF* (Hs00171455), *IL8* (Hs00174103), *GAPDH* (Hs02758991), *ACTIN* (Hs00357333), and *TUBULIN* (Hs00733770).

Protein Detection

Cell lysates for Western blotting were made in MPER (Thermo Scientific) lysis buffer with protease inhibitor cocktail (Roche). Protein (20 μg) was separated on 4%–20% Tris-HCl gel and then transferred onto a nitrocellulose membrane. Western blots were probed with antibodies against phospho-ERK1/2 T202/Y204 (Cell Signaling Technologies; CST #4695), ERK1/2 Cat #9107 (CST #4695), phospho-RSK T359/S363 (Millipore #04-419), RSK (BD Bioscience #610226), phospho-MEK1/2 S217/S221 (CST #9154), MEK1/2 (CST #9126), phospho-AKT S473 (CST #9271), AKT (CST #9272), phospho-BRAF S445 (CST #2696), BRAF (CST #9433), phospho-CRAF S289/S296/S301 (CST #9431), CRAF (CST #9422), PDGFRB (CST #4664), IGF1RB (CST 3027), GAPDH (Millipore #CB1001), and Actin (CST #4967).

ERK2 IMAP Enzymatic Assay

SCH772984 was tested in 8-point dilution curves in duplicate against purified ERK1 or ERK2. The enzyme was added to the reaction plate and incubated with the compound before adding a solution of substrate peptide and ATP. Fourteen microliters of diluted enzyme (0.3 ng active ERK2 per reaction) was added to each well of a 384-well plate. The plates were gently shaken to mix the reagents and incubated for 45 minutes at room temperature. The reaction was stopped with 60 μL of IMAP Binding Solution (1:2,200 dilutions of IMAP beads in 1× binding buffer). The plates were incubated at room temperature for an additional 0.5 hours to allow complete binding of phosphopeptides to the IMAP beads. Plates were read on the LJL Analyst (LJL BioSystems).

Cell-Cycle Analysis by Fluorescence-Activated Cell Sorting

Cell-cycle analysis was conducted by propidium iodide (PI) staining. LOX cells were collected after trypsinization, washed in PBS, and centrifuged for 2 minutes at 1,500 × *g*. The cells were resuspended and fixed in 70% ethanol for at least 30 minutes on ice or overnight at −20°C. The cell pellets were washed with PBS and resuspended in 0.5 mL of PI (50 μg/mL)/0.1% Triton X-100 solution containing RNase and incubated at room temperature in the dark for 30 minutes. The PI-stained cells were analyzed on a Becton Dickinson FACSCalibur flow cytometer. The cell-cycle profile was determined using both CellQuest (Becton Dickinson) and ModFit 3.0 (Verity Software). CellQuest was used to acquire data and also determine the percentage of cells in the sub-G_1 population. ModFit 3.0 software was used to determine the percentage of cells in G_1, S, and G_2.

Xenograft Tumor Growth Assay

Nude mice were injected subcutaneously with specific cell lines, grown to approximately 100 mm^3, randomized to treatment groups (10 mice/group), and treated intraperitoneally with either SCH772984 or vehicle according to the dosing schedule indicated in the figure legends. Tumor length (L), width (W), and height (H) were measured during and after the treatment periods by a caliper twice weekly on each mouse and then used to calculate tumor volume using the formula $(L \times W \times H)/2$. Animal body weights were measured on the same days twice weekly. Data were expressed as mean ± SEM. Upon completion of the experiment, vehicle- and SCH772984-treated tumor biopsies were processed for Western blot analysis.

Kinase Panel Screening

The kinase inhibitory profile of SCH772984 was evaluated over a 310-kinase panel at Invitrogen.

TdF Assay

The unfolding of rat ERK2, rat phosphorylated ERK2, and human MEK1 proteins was conducted at a final concentration of 0.5 μmol/L each in the TdF assay buffer (10 mmol/L HEPES pH 7.4, 150 mmol/L NaCl, 5 mmol/L $MgCl_2$, 1 mmol/L DTT) containing a final concentration of 5× Sypro Orange reporter dye. The samples contained 10, 5, or 2.5 μmol/L compound at a final DMSO concentration of 2%. Samples were run in 5 μL in a white 384-well real-time PCR plate (Roche Applied Science). The plates were sealed with a clear sealing film (Roche Applied Science) and assayed in the LightCycler 480-II (Roche Applied Science). The temperature was ramped from 23°C to 99°C in 15 minutes. The fluorescent intensity was collected at 15 data points per degree with excitation at 465 nm and emission at 580 nm.

Disclosure of Potential Conflicts of Interest

E.J. Morris is employed as an associate principal scientist at Merck Research Laboratories and has ownership interest (including patents) in Merck. C.R. Restaino is employed as a scientist at Merck Research Laboratories and has ownership interest (including patents) in Merck & Co./MSD. S. Black is employed as a senior scientist at Merck Research Laboratories. D. Hicklin has ownership interest (including patents) in Merck. No potential conflicts of interest were disclosed by the other authors.

Published OnlineFirst April 24, 2013; DOI: 10.1158/2159-8290.CD-13-0070

Authors' Contributions

Conception and design: E.J. Morris, S. Jha, C.R. Restaino, P. Dayananth, H. Zhu, A. Cooper, Y. Deng, B. Long, W. Windsor, L. Xiao, G. Shipps, X. Gao, L. Zhu, U. Philippar, P. Kirschmeier, W.R. Bishop, D. Hicklin, L. Zawel, S.E. Fawell, A.A. Samatar

Development of methodology: E.J. Morris, S. Jha, C.R. Restaino, P. Dayananth, A. Cooper, R. Zhang, M.H. Angagaw, J. Desai, L. Xiao, G. Shipps, J. Kelly, S. Paliwal, X. Gao, B.S. Babu, L. Zhu, P. Kirschmeier, D. Hicklin, L. Zawel, S.E. Fawell, A.A. Samatar

Acquisition of data (provided animals, acquired and managed patients, provided facilities, etc.): E.J. Morris, S. Jha, C.R. Restaino, P. Dayananth, A. Cooper, D. Carr, W. Jin, S. Black, B. Long, J. Liu, E. DiNunzio, S. Zhao, M.H. Angagaw, J. Wang, X. Gao, L. Zhu, P. Siliphaivanh, P. Kirschmeier, A.A. Samatar

Analysis and interpretation of data (e.g., statistical analysis, biostatistics, computational analysis): E.J. Morris, S. Jha, C.R. Restaino, P. Dayananth, H. Zhu, A. Cooper, D. Carr, B. Long, E. DiNunzio, W. Windsor, R. Zhang, E.M. Pinheiro, L. Xiao, G. Shipps, A. Hruza, J. Wang, X. Gao, B.S. Babu, L. Zhu, L. Zhang, M.R. Pelletier, P. Kirschmeier, D. Hicklin, L. Zawel, S.E. Fawell, A.A. Samatar

Writing, review, and/or revision of the manuscript: E.J. Morris, S. Jha, H. Zhu, Y. Deng, S. Black, B. Long, W. Windsor, R. Zhang, E.M. Pinheiro, L. Xiao, L. Zhang, B.A. Lutterbach, M.R. Pelletire, U. Philippar, D. Witter, W.R. Bishop, D. Hicklin, D.G. Gilliland, L. Jayaraman, L. Zawel, S.E. Fawell, A.A. Samatar

Administrative, technical, or material support (i.e., reporting or organizing data, constructing databases): E.J. Morris, S. Jha, J. Kelly, P. Daublain, A.A. Samatar

Study supervision: E.J. Morris, B. Long, W. Windsor, E.M. Pinheiro, G. Shipps, L. Zhu, L. Zhang, P. Kirschmeier, D. Hicklin, L. Jayaraman, L. Zawel, S.E. Fawell, A.A. Samatar

Acknowledgments

The authors thank Drs. Gary O'Neill, Ronald Doll, Neng-Yang Shih, and John Piwinsky for their support. This article is dedicated to the memory of our wonderful colleague, Linda James, who was a member of the ERK inhibitor program.

Grant Support

This work was supported by Merck Research Laboratories.

Received February 18, 2013; revised April 4, 2013; accepted April 13, 2013; published OnlineFirst April 24, 2013.

REFERENCES

1. Flaherty KT, Infante JR, Daud A, Gonzalez R, Kefford RF, Sosman J, et al. Combined BRAF and MEK inhibition in melanoma with BRAF V600 mutations. N Engl J Med 2012;367:1694–703.
2. Flaherty KT, Hodi FS, Fisher DE. From genes to drugs: targeted strategies for melanoma. Nat Rev Cancer 2012;12:349–61.
3. Little AS, Smith PD, Cook SJ. Mechanisms of acquired resistance to ERK1/2 pathway inhibitors. Oncogene 2013;32:1207–15.
4. Chapman PB, Hauschild A, Robert C, Haanen JB, Ascierto P, Larkin J, et al. Improved survival with vemurafenib in melanoma with BRAF V600E mutation. N Engl J Med 2011;364:2507–16.
5. Flaherty KT, Robert C, Hersey P, Nathan P, Garbe C, Milhem M, et al. Improved survival with MEK inhibition in BRAF-mutated melanoma. N Engl J Med 2012;367:107–14.
6. Hauschild A, Grob JJ, Demidov LV, Jouary T, Gutzmer R, Millward M, et al. Dabrafenib in BRAF-mutated metastatic melanoma: a multicentre, open-label, phase 3 randomised controlled trial. Lancet 2012;380:358–65.
7. Flaherty KT, Yasothan U, Kirkpatrick P. Vemurafenib. Nat Rev 2011; 10:811–2.
8. Lemech C, Infante J, Arkenau HT. The potential for BRAF V600 inhibitors in advanced cutaneous melanoma: rationale and latest evidence. Ther Adv Med Oncol 2012;4:61–73.
9. Greger JG, Eastman SD, Zhang V, Bleam MR, Hughes AM, Smitheman KN, et al. Combinations of BRAF, MEK, and PI3K/mTOR inhibitors overcome acquired resistance to the BRAF inhibitor GSK2118436 dabrafenib, mediated by NRAS or MEK mutations. Mol Cancer Ther 2012;11:909–20.
10. Shi H, Moriceau G, Kong X, Lee MK, Lee H, Koya RC, et al. Melanoma whole-exome sequencing identifies (V600E)B-RAF amplification-mediated acquired B-RAF inhibitor resistance. Nat Commun 2012;3:724.
11. Annis DA, Cheng CC, Chuang CC, McCarter JD, Nash HM, Nazef N, et al. Inhibitors of the lipid phosphatase SHIP2 discovered by high-throughput affinity selection-mass spectrometry screening of combinatorial libraries. Comb Chem High Throughput Screen 2009;12:760–71.
12. Aronov AM, Tang Q, Martinez-Botella G, Bemis GW, Cao J, Chen G, et al. Structure-guided design of potent and selective pyrimidylpyrrole inhibitors of extracellular signal-regulated kinase (ERK) using conformational control. J Med Chem 2009;52:6362–8.
13. Hatzivassiliou G, Liu B, O'Brien C, Spoerke JM, Hoeflich KP, Haverty PM, et al. ERK inhibition overcomes acquired resistance to MEK inhibitors. Mol Cancer Ther 2012;11:1143–54.
14. Pratilas CA, Solit DB. Targeting the mitogen-activated protein kinase pathway: physiological feedback and drug response. Clin Cancer Res 2010;16:3329–34.
15. Dougherty MK, Muller J, Ritt DA, Zhou M, Zhou XZ, Copeland TD, et al. Regulation of Raf-1 by direct feedback phosphorylation. Mol Cell 2005;17:215–24.
16. Alcala AM, Flaherty KT. BRAF inhibitors for the treatment of metastatic melanoma: clinical trials and mechanisms of resistance. Clin Cancer Res 2012;18:33–9.
17. Emery CM, Vijayendran KG, Zipser MC, Sawyer AM, Niu L, Kim JJ, et al. MEK1 mutations confer resistance to MEK and B-RAF inhibition. Proc Natl Acad Sci U S A 2009;106:20411–6.
18. Poulikakos PI, Persaud Y, Janakiraman M, Kong X, Ng C, Moriceau G, et al. RAF inhibitor resistance is mediated by dimerization of aberrantly spliced BRAF(V600E). Nature 2011;480:387–90.
19. Corcoran RB, Dias-Santagata D, Bergethon K, Iafrate AJ, Settleman J, Engelman JA. BRAF gene amplification can promote acquired resistance to MEK inhibitors in cancer cells harboring the BRAF V600E mutation. Sci Signal 2010;3:ra84.
20. Wagle N, Emery C, Berger MF, Davis MJ, Sawyer A, Pochanard P, et al. Dissecting therapeutic resistance to RAF inhibition in melanoma by tumor genomic profiling. J Clin Oncol 2011;29:3085–96.
21. Wang H, Daouti S, Li WH, Wen Y, Rizzo C, Higgins B, et al. Identification of the MEK1(F129L) activating mutation as a potential mechanism of acquired resistance to MEK inhibition in human cancers carrying the B-RafV600E mutation. Cancer Res 2011;71:5535–45.
22. Corcoran RB, Ebi H, Turke AB, Coffee EM, Nishino M, Cogdill AP, et al. EGFR-mediated re-activation of MAPK signaling contributes to insensitivity of BRAF mutant colorectal cancers to RAF inhibition with vemurafenib. Cancer Discov 2012;2:227–35.
23. Kim KB, Kefford R, Pavlick AC, Infante JR, Ribas A, Sosman JA, et al. Phase II study of the MEK1/MEK2 inhibitor Trametinib in patients with metastatic BRAF-mutant cutaneous melanoma previously treated with or without a BRAF inhibitor. J Clin Oncol 2013;31:482–9.
24. Shi H, Kong X, Ribas A, Lo RS. Combinatorial treatments that overcome PDGFRbeta-driven resistance of melanoma cells to V600EB-RAF inhibition. Cancer Res 2011;71:5067–74.